



Lidar-Millimeter Wave Radar Information Fusion
Multi-Target Detection Based on Unscented
Kalman Filter and Covariance Intersection
Algorithm

Fan Le, Hong Mo and Yinghui Meng

EasyChair preprints are intended for rapid dissemination of research results and are integrated with the rest of EasyChair.

November 2, 2021

Lidar-millimeter wave radar information fusion multi-target detection based on unscented Kalman filter and covariance intersection algorithm

Fan Le

College of Electric and Information Engineering Changsha University of Science and Technology Changsha, China lefan199711@163.com

Hong Mo

College of Electric and Information Engineering Changsha University of Science and Technology Changsha, China mohong198@163.com

Yinghui Meng

College of Electric and Information Engineering Changsha University of Science and Technology Changsha, China mengyinghui96@163.com

Abstract—Aiming at the problems of missed detection of occluded vehicles and long-distance targets when using Lidar for target detection in intelligent driving vehicles, this paper proposes a lidar-millimeter wave radar information fusion multi-target detection method based on the unscented Kalman filter and the covariance intersection algorithm. According to the data collected by the sensor, the UKF is used to generate the state estimation, and the CI algorithm is used to form the state estimation into a fusion state estimation. The effectiveness of the method is verified by Matlab simulation experiments, and compared with the algorithm based on Joint Probabilistic Data Association (JPDA) and Gaussian mixture probability hypothesis density (GMPHD) algorithm. The result is UKF-CI algorithm has higher accuracy for multi-target detection, and the effect is more obvious.

Keywords—Information fusion, Unscented Kalman filter algorithm, Covariance Intersection Algorithm, Multi-target detection

I. INTRODUCTION

Intelligent driving is an important development trend of the current automotive industry[1-3]. With the continuous update of various intelligent assisted driving systems, intelligent driving is moving rapidly towards unmanned driving[4]. The prerequisite for unmanned driving is to be able to accurately perceive the external environment Which can provide accurate and reliable information for the decision-making and vehicle control parts of the unmanned driving system, thereby improving the safety and stability of the unmanned driving system[5].

Lidar has high detection accuracy and wide detection range. It can accurately model surrounding obstacles, but is susceptible to weather and environmental influences, such as rain, snow, haze, sandstorms and other severe weather that block the laser beam, causing missed targets. Millimeter wave radar is not affected by weather and light and is sensitive to metals such as vehicles. It has a longer detection range and can penetrate fog, dust, and vegetation to detect vehicles. However, millimeter wave radar is inferior to lidar in detection accuracy[6-9].The sensing ability of a single sensor is limited, and multi-target detection based on multi-sensor fusion will become the main method. If the two are fused for target detection, the problems of missed detection caused by vehicle occlusion and inaccurate target detection accuracy under severe weather can be solved. Sensor fusion is mainly divided into three types: information-level fusion, feature-level fusion, and decision-level fusion.Literature [10] studied the multi-sensor data fusion positioning technology

of the Kalman filter (KF) model. The data was preprocessed by KF, and the preprocessing confidence and accuracy were evaluated by calculating the relative error and the root mean square error. Finally, The optimal weighted fusion estimation algorithm is used to fuse the filtering results, and the results show that the accuracy of navigation and positioning is improved.Literature [11] applies Kalman consensus filtering to target tracking, but the KF algorithm is only very effective in processing linear systems, and the processing effect for nonlinear systems is very poor.Literature [12] utilizes the extended Kalman filter (EKF) information fusion technology and applies it to vehicle state estimation, and realizes the use of a small amount of easily measurable vehicle state information fusion to obtain the required difficult-to-measure vehicle state. There is a certain degree of accuracy in vehicle state estimation.However, the EKF algorithm is based on the first-order Taylor series expansion of the first-order nonlinear system, and usually has good processing results for the first-order nonlinear system and the low-order nonlinear system, and the processing effect for the high-order nonlinear system is poor.Therefore, literature [13] proposed a passive multi-sensor fusion tracking based on unscented Kalman filter, which uses a tracking strategy of centralized fusion of multiple passive sensors to achieve multi-sensor fusion, and proves that it has higher-order accuracy than EKF. UKF is an approximation of the probability density of a nonlinear function. It does not need to calculate the Jacobian matrix. It can usually reach the second to third order accuracy. It can effectively improve the low estimation accuracy and stability of the KF and EKF algorithms in the nonlinear system[14-15].

In response to the above problems, this paper proposes a laser-millimeter wave radar fusion multi-target detection method based on the unscented Kalman filter and the covariance intersection algorithm. The UKF algorithm is used to process the data collected by the sensor to obtain the target state estimation. The CI algorithm fuses the target state estimation of millimeter wave radar and lidar, calculates and outputs the fusion state estimation, and this paper introduces the Generalized optimal subpattern assignment [16](GOSPA) algorithm in the experiment to compare the accuracy of UKF-CI with JPDA[17] and GM-PHD[18] algorithms for target detection. The GOSPA index is used to quantitatively evaluate the algorithm's omission detection and error detection at each time step. A lower index indicates a better tracking accuracy.

II. THEORETICAL BASIS

A. System model

In order to better fit the actual traffic scene, this paper chooses the "Constant Turning Rate and Speed Magnitude Model (CTRV)" as the system model of this paper. The state equation is

$$x_{k+1} = x_k + \begin{bmatrix} \frac{s_k}{\theta_k} (\sin(\theta + \omega\Delta t) - \sin(\theta)) \\ \frac{s_k}{\theta_k} (-\cos(\theta + \omega\Delta t) + \cos(\theta)) \\ 0 \\ \omega\Delta t \\ 0 \end{bmatrix} + \begin{bmatrix} \frac{1}{2}(\Delta t)^2 \cos(\theta)v_{a,k} \\ \frac{1}{2}(\Delta t)^2 \sin(\theta)v_{a,k} \\ \Delta tv_{a,k} \\ \frac{1}{2}(\Delta t)^2 v_{\dot{\omega},k} \\ \Delta tv_{\dot{\omega},k} \end{bmatrix} \quad (1)$$

In formula (1): $x_k = [x, y, s, \theta, \omega]^T$, x is the x coordinate position, y is the y coordinate position, s is the linear velocity, θ is the deflection angle, ω is the angular velocity; $\Delta t = t_{k+1} - t_k$ is the time interval; $v_k = [v_{a,k}, v_{\dot{\omega},k}]^T$ is the Gaussian white noise with the mean value of 0, $v_{a,k}$ is the longitudinal acceleration noise, $v_{a,k} \sim N(0, \sigma_a^2)$, and $v_{\dot{\omega},k}$ is the angular acceleration noise, $v_{\dot{\omega},k} \sim N(0, \sigma_{\dot{\omega}}^2)$. Meet the following conditions:

$$E[v_k] = 0 \quad (2)$$

$$Q_k = E\{v_k, v_k^T\} = \begin{bmatrix} \sigma_a^2 & 0 \\ 0 & \sigma_{\dot{\omega}}^2 \end{bmatrix} \quad (3)$$

In formula (2-3): E is the expectation; Q_k is the state noise covariance matrix. σ_a^2 is the longitudinal acceleration noise variance, $\sigma_{\dot{\omega}}^2$ is the angular acceleration noise variance.

The system measurement model is:

$$z_{k+1} = h(x_{k+1}) + \xi_{k+1} \quad (4)$$

$$z_{k+1} = [\rho, \beta, \dot{\rho}]^T \quad (5)$$

$$\rho = \sqrt{x^2 + y^2} \quad (6)$$

$$\beta = \arctan\left(\frac{y}{x}\right) \quad (7)$$

In formula (4-7): $h(x)$ is a non-linear transfer function, which can convert the predicted state space into a measurement state space; ρ , β , $\dot{\rho}$ is the position, deflection angle, and velocity observed by the radar; ξ_{k+1} is the pure accumulation of measurement errors, and the influence on the measurement results is determined by Measurement covariance noise R representation.

$$R = \begin{bmatrix} \sigma_\rho^2 & 0 & 0 \\ 0 & \sigma_\beta^2 & 0 \\ 0 & 0 & \sigma_{\dot{\rho}}^2 \end{bmatrix} \quad (8)$$

The measurement model in this article takes millimeter-wave radar measurement as an example. The lidar measurement is basically the same as the millimeter-wave radar update. The only difference is that there is no need to convert the prediction space to the measurement space, and there is no need for a non-linear conversion function $h(x)$.

B. Unscented Kalman filter algorithm

UKF is a nonlinear filtering method that uses unscented transformation to determine sampling near the estimated point. Unlike the extended Kalman filter (EKF), it is not a linear approximation of the nonlinear equation at the estimated point, but Use the Gaussian density represented by the sample points to approximate the probability density function of the state. In this way, for any nonlinear model, the mean and covariance of the model state can be accurate to the second order, and the error is only to the third order or even higher.

1) UKF initialization

Set initial values for the initial state of the target and the initial error covariance matrix:

$$\hat{x}_0 = E[x_0] \quad (9)$$

$$P_{x0} = E[(x_0 - \hat{x}_0)(x_0 - \hat{x}_0)^T] \quad (10)$$

Since the two-dimensional process noise vector is also non-linear, we will incorporate v_k into x_k for the convenience of calculation, augment the state vector $x_{a,k} = [x_k, v_{ak}, v_{\dot{\omega}k}]^T$.

$$x_{a,0} = E[x_{a,k}] = E[\hat{x}_0, 0, 0]^T \quad (11)$$

$$P_{a,0} = E[(x_{a,0} - \hat{x}_{a,0})(x_{a,0} - \hat{x}_{a,0})^T] = \begin{bmatrix} P_{x0} & 0 \\ 0 & Q \end{bmatrix} \quad (12)$$

Among them: $P_{a,0}$ is the augmented error covariance matrix of the system model.

2) Predict

Calculate $2N+1$ sigma points, that is, sampling points, where N refers to the dimension of the state.

$$\begin{cases} M_{a,k|k} = x_{a,k|k} \\ M_{a,k|k}^{[i]} = x_{a,k|k} + (\sqrt{(N+\lambda)P_{a,k|k}})_i, i=1,2,\dots,N \\ M_{a,k|k}^{[i]} = x_{a,k|k} - (\sqrt{(N+\lambda)P_{a,k|k}})_{i-N}, i=N+1, N+2, \dots, 2N \end{cases} \quad (13)$$

In formula (13): $x_{a,k|k}$ and $P_{k|k}$ are the estimated value of the time k sensor and the estimated error covariance matrix respectively; $M_{a,k|k}^{[i]}$ is the sigma point; λ is the scale factor; The best value of λ is $3-N$. The weight of the sampling point is

$$\omega_m^{(0)} = \frac{\lambda}{N + \lambda} \quad (14)$$

$$\omega_m^{(i)} = \frac{\lambda}{2(N + \lambda)}, i = 1, 2, \dots, 2N \quad (15)$$

$$x_{a,k+1|k} = \sum_{n=0}^{2N} \omega_m^{(i)} M_{a,k+1|k} \quad (16)$$

$$P_{a,k+1|k} = \sum_{n=0}^{2N} \omega_m^{(i)} (x_{a,k+1|k} - M_{a,k+1|k})(x_{a,k+1|k} - M_{a,k+1|k})^T + Q \quad (17)$$

In formula (16-17): $x_{a,k+1|k}$ represents the update prediction of the state space sigma point set; $P_{a,k+1|k}$ represents the update prediction error covariance of the system state.

3) Measurement update

First, after linear transformation of the millimeter wave radar observation equation. Calculate the measurement prediction value and the mean value of the measurement prediction obtained by weighted summation.

$$Z_{k+1|k} = h[M_{a,k+1|k}] \quad (18)$$

$$z_{k+1|k} = \sum_{n=0}^{2N} \omega_m^{(i)} Z_{k+1|k} \quad (19)$$

$$P_{z,k+1|k} = \sum_{n=0}^{2N} \omega_m^{(i)} (Z_{k+1|k} - z_{k+1|k})(Z_{k+1|k} - z_{k+1|k})^T + R \quad (20)$$

$$P_{x,z} = \sum_{n=0}^{2N} \omega_m^{(i)} (M_{a,k+1|k} - z_{k+1|k})(M_{a,k+1|k} - z_{k+1|k})^T \quad (21)$$

In formula (18-21): $Z_{k+1|k}$ is the measurement update value of the sigma point set in the measurement space; $z_{k+1|k}$ is the mean value of the measurement prediction obtained by weighted summation; $P_{z,k+1|k}$ is the measurement covariance matrix; $P_{x,z}$ is the cross covariance matrix of measurement and prediction.

Calculate the Kalman gain:

$$K_{k+1|k} = P_{x,z} P_{z,k+1|k}^{-1} \quad (22)$$

The status update value and covariance update are as follows:

$$x_{k+1|k+1} = x_{k+1|k} + K_{k+1|k} (z_{k+1} - z_{k+1|k}) \quad (23)$$

$$P_{k+1|k+1} = P_{k+1|k} - K_{k+1|k} P_{z,k+1|k} K_{k+1|k}^T \quad (24)$$

In formula (23-24): $x_{k+1|k+1}$ represents the estimated value of the system state update, and $P_{k+1|k+1}$ represents the updated covariance.

C. CI algorithm

The sampling and transmission rate of each sensor in the multi-sensor fusion technology is different, so the calculation of the covariance matrix in the state estimation is extremely complicated and does not conform to the real scene, and the CI algorithm only uses the state estimation and the state estimation covariance to generate fusion estimation does not need to calculate the cross-covariance matrix, which can reduce the complexity of the calculation, so that the calculation efficiency of the system is faster.

In the fusion gap $(t_k, t_{k+1}]$, the fusion estimate and covariance are

$$P_{k+1} = \sum_{b=1}^2 X_b [P_{b,k+1|k+1}]^{-1} \quad (25)$$

$$x_{k+1} = P_{k+1} \sum_{b=1}^2 X_b [P_{b,k+1|k+1}]^{-1} x_{b,k+1|k+1} \quad (26)$$

In formula (17-18), $X_b, b = \{1, 2\}$ represents the weight coefficient of millimeter wave radar and lidar, X_1 represents millimeter wave radar, and X_2 represents lidar.

According to the optimality in the sense of mean square error, that is $X_b : \min \{tr[P_{k+1}], b = 1, 2\}$.

$$\sum_{b=1}^2 X_b = 1 \quad (27)$$

The weight coefficient is determined by the corresponding diagonal term in the suboptimal method for real-time consideration, namely

$$X_b = \frac{1}{\frac{tr[P_{k+1}]}{tr[P_{k+1}]}} \quad (28)$$

III. EXPERIMENTAL VERIFICATION

A. Experimental scene setting

In order to verify the effectiveness of the algorithm in this paper, experiments are carried out in Matlab software. First, use the Driving Scenario Designer in Matlab to build the experimental scene. The experimental scene diagram is shown in Figure 1 below. From the picture, this article builds a 400-meter-long three-lane highway with scenes such as overtaking, following, and changing lanes. The target description in this article takes millimeter wave radar detection as an example. $R = \{R1, R2, R3, R4, R5, R7\}$ a car target and $R6$ a truck target. $R1-R7$ are the detection results of the millimeter wave radar at the current moment. $R1, R3$ and $R6$ are the lane-keeping vehicles in the experimental scene. $R2$ is the lane-changing vehicle in the experimental scene. $R4$ is the overtaking part of the vehicle in the experimental scene. $R5$ is a tracking vehicle for ego vehicles. $R7$ is a vehicle that was missed by lidar because it was blocked by $R5$. Follow-up $R7$ will change the road and be detected by lidar. $F1-F6$ are the lidar detection results at

the current moment. Ego vehicle radar settings are shown in Table I.

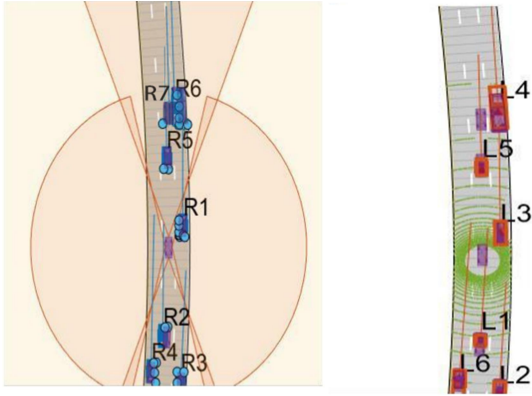


Fig. 1. Experimental scene setting diagram

TABLE I. RADAR PARAMETER SETTING TABLE

| | Lidar | Radar | Radar |
|----------------------|-------|--------------|--------------|
| quantity | 1 | 2 | 2 |
| Location | top | Left & right | Front & rear |
| Azimuth | 360° | 150° | 45° |
| Elevation | 40° | — | — |
| Azimuth resolution | 0.2° | 6° | 6° |
| Elevation resolution | 1.25° | — | — |
| Elevation channel | 32 | — | — |

B. Analysis of results

The simulation experiment is compared with JPDA algorithm and GM-PHD algorithm. Both JPDA and GM-PHD algorithm are commonly used multi-target detection algorithms. The simulation parameter settings are shown in Table II below. This article runs the simulation program to get the following experimental results, as shown in Figure 2-5.

TABLE II. SIMULATION PARAMETER SETTING TABLE

| Simulation parameters | Value |
|------------------------------|-------------|
| State noise covariance | $10^{-3} I$ |
| Measurement noise covariance | $10^{-3} I$ |
| Data collection cycle | 0.1s |

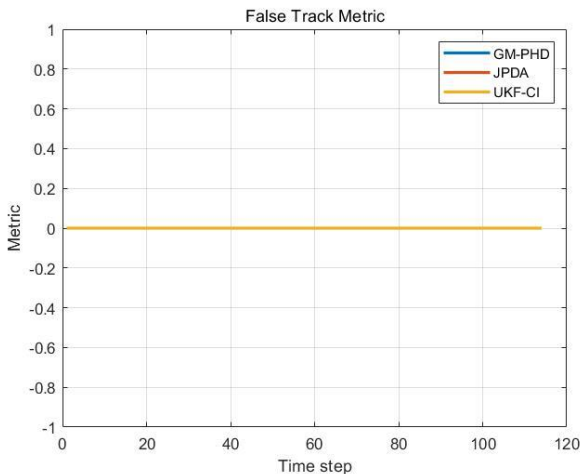


Fig. 2. False tracking result graph

Figure 2 shows the result of false tracking. From the figure, it can be seen that GOSPA's error tracking indicators are all 0, which means that none of the three algorithms has error detection during the experiment.

Figure 3 shows the results of GOSPA algorithm after scoring JPDA, GM-PHD and UKF-CI algorithms. As shown in Figure 2 that none of the three algorithms have error detection, the GOSPA indicator in Figure 3 represents the target missed detection or the positioning error caused by the state estimation of each vehicle. It can be seen from Figure 3 that the GOSPA index of the UKF-CI algorithm at each time step is lower than that of the JPDA and GM-PHD algorithms. It can be concluded that the detection result of UKF-CI algorithm is better than JPDA and GM-PHD algorithm. The target detection accuracy of the UKF-CI algorithm is higher than that of the JPDA and GM-PHD algorithms. This can prove the effectiveness of the UKF-CI algorithm.

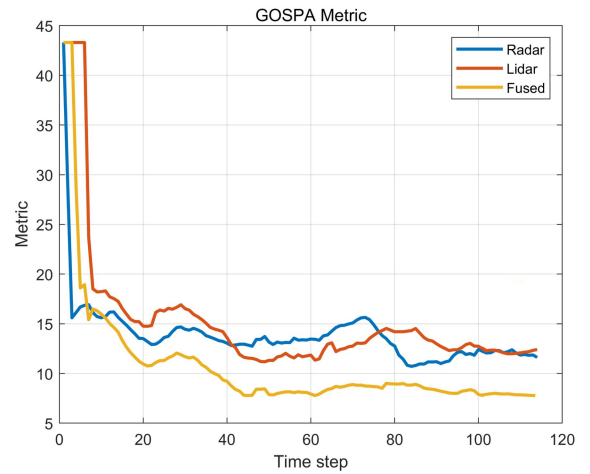


Fig. 3. Comparison of target detection results

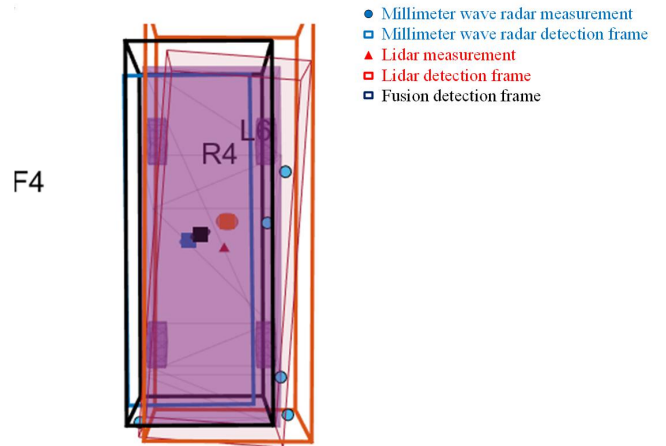


Fig. 4. The effect of R4 being detected at a certain moment

Figure 4 is the detection result diagram of the detected vehicle R4 at a certain moment. It can be seen from the figure that the vehicle detection frame generated after the measurement values of Lidar and millimeter wave radar and the estimation of JPDA and GM-PHD algorithms are all deviated from the true state of the R4 vehicle. The vehicle detection frame generated by the UKF-CI fusion algorithm has a small deviation from the real state. It proves once again that the accuracy of the UKF-CI algorithm is high.

Figure 5 below shows the effect of the fusion algorithm on multi-target detection. It can be seen from the results in the figure that the UKF-CI fusion algorithm can accurately detect 6 car targets and 1 truck target, and can accurately track them. From the results shown in the figure, it can be seen that the fusion algorithm can accurately detect each target. And comparing Fig. 5 with Fig. 1, it can be seen that $R7$ in Fig. 1 and $F7$ in Fig. 5 are the same target, which was missed by the lidar. Therefore, this method can not only accurately detect multiple targets, but also effectively solve the problem of lidar missed detection due to occlusion.

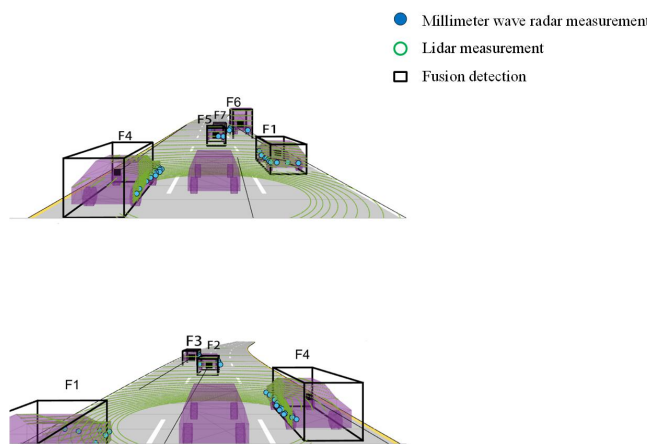


Fig. 5. Multi-target detection effect diagram

IV. CONCLUSION

In this paper, based on the unscented Kalman filter algorithm, the innovative fusion covariance intersection algorithm makes the UKF do not need to calculate the advantage of the cross-covariance matrix, and proposes a lidar-millimeter wave radar information fusion multi-target detection based on unscented Kalman filter and covariance intersection algorithm. Simplify the complexity of the system calculation, make the calculation efficiency of the system faster. Fully combining the advantages of millimeter wave radar and lidar, it solves the problem that lidar misses detection targets due to occlusion, and can accurately detect all surrounding vehicles and realize accurate perception of the external environment. It provides a reliable and accurate information source for the subsequent decision-making and control links of unmanned vehicles, which is conducive to improving the safety of the entire driving system. The experimental results in this article verify the effectiveness of the proposed method and prove that the UKF-CI algorithm is superior to the JPDA algorithm-based lidar target detection method and the millimeter-wave radar target detection method based on the GM-PHD algorithm. Considering that this article only sets up experiments in a simulation environment, and does not include pedestrians, obstacles and other traffic participants in the real environment in the experimental scenes, the follow-up work will use the sensor data of the real scenes to further verify the effectiveness of the algorithm in the real environment.

V. REFERENCES

- [1] Huang Xiaoping, Wang Yan, Miao Pengcheng. Principle and application of target location and tracking-MATLAB simulation[M]. Beijing: Electronic Industry Press, 2018.
- [2] Hu Yunfeng, Qu Ting, Liu Jun, Shi Zhuqing, Zhu Bing, Cao Dongpu, Chen Hong. Research status and prospects of human-machine collaborative control of smart cars[C]. Acta Automatica Sinica, 2019, 45(7): 1261-1280.
- [3] Tasaki T. Perception and Decision Making for the Autonomous Driving System[C]. 2018 International Symposium on Micro-NanoMechatronics and Human Science (MHS). IEEE, 2019, pp.1-3.
- [4] You Dingyi, Wang Haiyan, Yang Kaiming. State-of-the-art and trends of autonomous driving technology[C]. 2018 IEEE International Symposium on Innovation and Entrepreneurship. 2018, pp.1-8.
- [5] Zhang Yanhui, Xu Kun, Zheng Chunhua, Feng Wei, Xu Guoqing. Advanced research on information perception technologies of intelligent electric vehicles[J]. Chinese Journal of Scientific Instrument, 2017, 38(4): 794-805.
- [6] D. Göhring, M. Wang, M. Schnürmacher and T. Ganjineh, Radar/Lidar sensor fusion for car-following on highways[C]. The 5th International Conference on Automation, Robotics and Applications, 2011, pp.407-412.
- [7] Hajiri H, Rahal M C. Real Time Lidar and Radar High-Level Fusion for Obstacle Detection and Tracking with evaluation on a ground truth[J]. International Journal of Mechanical & Mechatronics Engineering, 2018, 140(8): 821.
- [8] Lee H, Chae H, Yi K. A Geometric Model based 2D LiDAR/Radar Sensor Fusion for Tracking Surrounding Vehicles[J]. IFAC Papers OnLine, 2019, 52(8): 130-135.
- [9] H. Cho, Y. Seo, B. V. K. V. Kumar and R. R. Rajkumar. A multi-sensor fusion system for moving object detection and tracking in urban driving environments[C]. 2014 IEEE International Conference on Robotics and Automation (ICRA), 2014, pp.1836-1843.
- [10] Song Zhihui, Zhao Yanxiao. Modeling and simulation of multi-sensor data fusion navigation and positioning based on Kalman filter model[J]. Digital Communication World, 2019(9): 62-63, 73.
- [11] Liu Qinyuan, Wang Zidong, He Xiao, D.H. Zhou. On Kalman-consensus filtering with random link failures over sensor networks[J]. IEEE Transactions on Automatic Control, 2018, 63(8): 2701-2708.
- [12] Zong Changfu, Pan Zhao, Hu Dan, et al. Application of Information Fusion Technology Based on Extended Kalman Filter in Vehicle State Estimation[J]. Chinese Journal of Mechanical Engineering, 2009, 45(010): 272-277.
- [13] Yang Baisheng, Ji Hongbing. Passive multi-sensor fusion tracking based on unscented Kalman filter[J]. Control and Decision, 2008, 23(4): 460-463.
- [14] Yan Liping, Xia Yuanqing, Liu Baosheng, Fu Meng. Multi-sensor optimal estimation theory and application[M]. Beijing: Science Press, 2014: 108-124.
- [15] Jiang Zhiyu, Guo Chengjun. Application comparison of unscented Kalman filter and unscented particle filter in initial alignment of INS[J]. Science Technology and Engineering, 2018, 18(7): 267-270.
- [16] A. S. Rahmathullah, Á. F. García-Fernández and L. Svensson. Generalized Optimal Sub-Pattern Assignment Metric[C]. 20th International Conference on Information Fusion (Fusion), 2017, pp.1-8.
- [17] Wang Guicheng, Chuang Feng, Tao Junwei, Ran Mo and Zhang Min. Research on multi-maneuvering target tracking JPDA algorithm[C]. 2018 Chinese Control And Decision Conference (CCDC), 2018, pp.3558-3561.
- [18] Shen Tuhua, Xue Anke, Zhou Zhili. Multi-sensor Gaussian mixture PHD fusion multi-target tracking method[J]. Acta Automatica Sinica, 2017, 43(6): 1028-1037.